Check for updates

Received: 8 September 2022 | Revised: 8 February 2023 | Accepted: 16 March 2023

DOI: 10.1111/gcb.16740

Global Change Biology WILEY

RESEARCH ARTICLE

The energy–water limitation threshold explains divergent drought responses in tree growth, needle length, and stable isotope ratios

Joan Dudney[1,2] | Andrew M. Latimer[3] | Phillip van Mantgem[4] | Harold Zald[5] | Claire E. Willing[6,7] | Jonathan C. B. Nesmith[8] | Jennifer Cribbs[3] | Elizabeth Milano[4,9]

[1]Environmental Studies Program, Santa Barbara, California, USA

[2]Bren School of Environmental Science & Management, UC Santa Barbara, Santa Barbara, California, USA

[3]Department of Plant Sciences, University of California, Davis, California, USA

[4]U.S. Geological Survey, Western Ecological Research Center, Sacramento, California, USA

[5]USDA Forest Service, Pacific Northwest Research Station, Corvallis, Oregon, USA

[6]Department of Biology, Stanford University, Stanford, California, USA

[7]School of Environmental and Forest Sciences, University of Washington, Seattle, Washington, USA

[8]USDA Forest Service, Pacific Northwest Research Station, Portland, Oregon, USA

[9]USDA Forest Service, Rocky Mountain Research Station, Moscow, Idaho, USA

Correspondence
Joan Dudney, Environmental Studies Program, 4312 Bren Hall, Santa Barbara, CA 93106, USA.
Email: dudney@ucsb.edu

Funding information
David H. Smith Conservation Fellowship; Hatch Project, Grant/Award Number: CA-D-PLS-2017-H; National Science Foundation

Abstract

Predicted increases in extreme droughts will likely cause major shifts in carbon sequestration and forest composition. Although growth declines during drought are widely documented, an increasing number of studies have reported both positive and negative responses to the same drought. These divergent growth patterns may reflect thresholds (i.e., nonlinear responses) promoted by changes in the dominant climatic constraints on tree growth. Here we tested whether stemwood growth exhibited linear or nonlinear responses to temperature and precipitation and whether stemwood growth thresholds co-occurred with multiple thresholds in source and sink processes that limit tree growth. We extracted 772 tree cores, 1398 needle length records, and 1075 stable isotope samples from 27 sites across whitebark pine's (*Pinus albicaulis* Engelm.) climatic niche in the Sierra Nevada. Our results indicated that a temperature threshold in stemwood growth occurred at 8.4°C (7.12–9.51°C; estimated using fall-spring maximum temperature). This threshold was significantly correlated with thresholds in foliar growth, as well as carbon ($\delta^{13}C$) and nitrogen ($\delta^{15}N$) stable isotope ratios, that emerged during drought. These co-occurring thresholds reflected the transition between energy- and water-limited tree growth (i.e., the E–W limitation threshold). This transition likely mediated carbon and nutrient cycling, as well as important differences in growth-defense trade-offs and drought adaptations. Furthermore, whitebark pine growing in energy-limited regions may continue to experience elevated growth in response to climate change. The positive effect of warming, however, may be offset by growth declines in water-limited regions, threatening the long-term sustainability of the recently listed whitebark pine species in the Sierra Nevada.

KEYWORDS
climate change, dendrochronology, ecohydrological classes, foliar nitrogen, forest productivity, photosynthesis, stable nitrogen isotopes, threshold responses, whitebark pine

1 | INTRODUCTION

Many studies predict that drought frequencies will increase in the future, leading to unprecedented shifts in carbon sequestration and forest composition (Allen et al., 2015; Cook et al., 2018; Trenberth et al., 2014). Though drought-induced growth declines and dieback have been widely documented across many terrestrial systems (Allen et al., 2010; Anderegg et al., 2020; Hammond et al., 2022), a number

© 2023 John Wiley & Sons Ltd. This article has been contributed to by U.S. Government employees and their work is in the public domain in the USA.

of studies in the Northern Hemisphere have reported highly divergent growth responses to the same drought (Hartl-Meier et al., 2014; Jolly et al., 2005). For example, high elevation forests experienced both positive and negative growth responses to extreme drought in Switzerland (Sturm et al., 2022) and South Tyrol, Italy (Lewińska et al., 2018). In Canadian boreal forests, the first year of drought led to the highest annual net ecosystem productivity measurements over a 9-year study period (Kljun et al., 2006). Reconciling these divergent drought responses and identifying the underlying mechanisms causing them are critical to quantify the impact of increased drought frequency in a warming world (Cook et al., 2018).

Divergent growth responses to drought may reflect the vegetation's primary climatic constraints. Two major classes of climatic limitation (or ecohydrological classes) include (1) water limited and (2) energy limited. Although the definitions of these classes are variable (Field et al., 2005; Roebroek et al., 2020; Stephenson, 1998; Whittaker et al., 2007), in water-limited systems, plant growth is often more responsive to changes in precipitation than temperature, as potential rates of evapotranspiration (PET) can greatly exceed precipitation inputs (Jenerette et al., 2012; Roebroek et al., 2020). In energy-limited systems, plant growth is often more responsive to changes in temperature than precipitation, as evapotranspiration is typically lower than precipitation inputs and the majority of precipitation falls as snow, thereby reducing the growing season (Hartl-Meier et al., 2014; Roebroek et al., 2020; Sánchez-Salguero et al., 2017; Stephenson, 1998; van der Maaten-Theunissen et al., 2013). At broad spatial scales, transitions from water-limited to energy-limited forests often occur across latitudinal and elevational gradients (Babst et al., 2019; Roebroek et al., 2020). Whether this transition is associated with threshold stemwood growth responses to drought, however, remains poorly understood.

A threshold is characterized by a discontinuity in an ecosystem response (e.g., growth or productivity) at a specific level of environmental pressure (Hillebrand et al., 2020). Although studies have captured contrasting stemwood temperature and drought responses across elevation, the estimated breakpoint (i.e., where stemwood drought responses shift from negative to positive) is highly variable, ranging from 800 to 3200 m (Hartl-Meier et al., 2014; Salzer et al., 2014; van der Maaten-Theunissen et al., 2013). Elevation is often correlated with many biotic and abiotic factors, making it difficult to parse the causal effects of climate on tree growth (Dudney et al., 2021; Reich, Rich, et al., 2014). Thus, it remains unclear if these elevation breakpoints correspond to the transition from water- to energy-limited systems and which climate variables are associated with the breakpoint.

In addition, few studies have tested whether the breakpoint in stemwood growth co-occurs with thresholds in physiological factors that limit tree growth. Across an aridity gradient, for example, thresholds in various ecosystem attributes, including soil fertility, plant productivity, specific leaf area, and leaf photosynthetic rates, were correlated with a major and abrupt shift in species richness (Berdugo et al., 2020). Stemwood is the product of many ecosystem processes, including source (i.e., photosynthesis) and sink (i.e., direct environmental controls on cambial cell development) factors that limit tree growth (Cabon et al., 2022; Muller et al., 2011). Although untested, the breakpoint in stemwood growth across elevation may be associated with abrupt shifts in source and sink processes affecting tree growth, including photosynthesis, leaf traits, and nutrient cycling.

As climatic controls on growth shift from water to energy limited, photosynthetic rates may change across ecohydrological classes, particularly during drought. In water-limited regions, relatively isohydric species, including pines, often close their stomata during drought to avoid hydraulic failure (McDowell et al., 2022). As a result, the ratio of the heavy to light carbon isotopes ($\delta^{13}C$) in leaves, which is primarily controlled by stomatal conductance and photosynthetic capacity (Buckley, 2005; Farquhar et al., 1989; Shestakova et al., 2017), often increases (becomes less negative) during drought (Klein, 2014; McDowell et al., 2008). In contrast, in energy-limited regions, stomatal closure has been linked to low soil and air temperatures (Mahalovich et al., 2016), which inhibit sap flow, thereby increasing water potential (Day et al., 1991; Delucia, 1986); water availability, however, is still likely a limiting resource when photosynthesis increases during spring and summer months (Day et al., 1989; Moyes et al., 2015). Thus, in energy-limited regions, higher temperatures during drought may lead to increased discrimination against ^{13}C, as the growing season is extended and atmospheric gas exchange increases (Shestakova et al., 2017). Though energy and water limitation have been linked to declines in stomatal conductance (Bucholz et al., 2020; Gessler et al., 2014; Hultine & Marshall, 2000; McDowell et al., 2022), whether thresholds in gas exchange during drought occur in response to the transition between energy- and water-limited systems is largely unknown.

In addition, leaf size can vary across climatic gradients, reflecting trade-offs between light capture and the probability of environmental stress (Marquis et al., 2020; Poorter et al., 2009; Reich, 2014). In water-limited systems, conifer needle length often decreases with lower water availability (Dobbertin et al., 2010; Guérin et al., 2018). Increased temperature, however, has a more variable effect, initiating earlier terminal budbreak at the beginning of the growing season—though not always (Adams et al., 2015)—and limiting growth later in the growing season (Olszyk et al., 1998). Conversely, in energy-limited systems, needle length is often positively correlated with temperature (Jankowski et al., 2017; Tyukavina et al., 2019; Zhai et al., 2012) while precipitation has a more variable and often decoupled effect (Jankowski et al., 2017; Ordoñez et al., 2009; Reich, Rich, et al., 2014; Tyukavina et al., 2019). These contrasting growth responses suggest that declines in precipitation will differentially impact leaf traits within energy- and water-limited systems, potentially leading to threshold effects during drought (Dudney et al., 2021).

Finally, the availability of organic nitrogen (N) for tree growth shifts across global temperature and precipitation gradients (Craine et al., 2009; Reich, Luo, et al., 2014). Although stable nitrogen isotope ratios ($\delta^{15}N$) integrate many complex N cycling processes (Robinson, 2001), at a global scale, foliar $\delta^{15}N$ often increases with mean annual temperature and declines with mean annual

13652486, 2023, 15, Downloaded from https://onlinelibrary.wiley.com/doi/10.1111/gcb.16740 by National Forest Service Library, Wiley Online Library on [03/08/2023]. See the Terms and Conditions (https://onlinelibrary.wiley.com/terms-and-conditions) on Wiley Online Library for rules of use; OA articles are governed by the applicable Creative Commons License

precipitation (Craine et al., 2009). Low temperatures limit N uptake by roots and lower decomposition and mineralization rates, which decrease available soil N (Hobbie et al., 2000; Kirschbaum, 1995). In systems that experience very low mean annual temperatures (MAT; MAT < −0.5°C), $\delta^{15}N$ may be the least responsive to changes in temperature (Craine et al., 2009), reflecting low N availability (Amundson et al., 2003) and the high dependence on mycorrhizal associations (Handley et al., 1999; Hobbie & Colpaert, 2003; Steidinger et al., 2019). In warmer regions, higher soil N likely leads to higher foliar $\delta^{15}N$, as rates of nitrification and mineralization are often greater and can be more responsive to temperature and precipitation (Larsen et al., 2011)—though not always (Auyeung et al., 2013). Furthermore, responsiveness in foliar $\delta^{15}N$ to temperature may increase as systems transition from energy-limited, N-depleted soils to water-limited, more nutrient-rich soils, though this hypothesis has never been tested.

To identify the transition from energy-limited to water-limited systems, we evaluated whether stemwood growth (ring-width index, RWI) exhibited nonlinear responses to temperature and precipitation. If the responses were nonlinear, we expected that the breakpoint in either temperature or precipitation would correspond to divergent growth responses during extreme drought, corroborating energy- and water-limited growth responses. Specifically, we hypothesized that stemwood growth would increase in response to drought below the energy–water limitation threshold (suggesting that growth is energy limited) and decrease in growth above the threshold (suggesting that growth is water limited; Figure 1). Because stemwood growth can be coupled with various source and sink processes, we expected that the transition from energy- to water-limited systems would co-occur with threshold responses in stable carbon isotope ratios ($\delta^{13}C$), needle length, and the abundance of foliar ^{15}N that emerged during extreme drought (Figure 1).

To test these hypotheses, we conducted a field study across the Sierra Nevada focused on whitebark pine (*Pinus albicaulis* Engelm.). The study included long-term growth measurements (tree cores; $n = 772$) that spanned multiple droughts (Figure 2b). We also included short-term needle growth ($n = 1398$) and stable carbon and nitrogen isotopes signatures ($n = 1075$) that spanned the most recent extreme drought of 2012–2015, as well as non-drought years (Robeson, 2015; Stephenson et al., 2019). We define drought as a major decline in precipitation relative to average conditions—that is, a meteorological drought—which is often associated with increases in temperature. Importantly, meteorological drought is defined independently of the corresponding impacts on vegetation, that is often captured in the definition of ecological drought (Lloyd-Hughes, 2014; Slette et al., 2019).

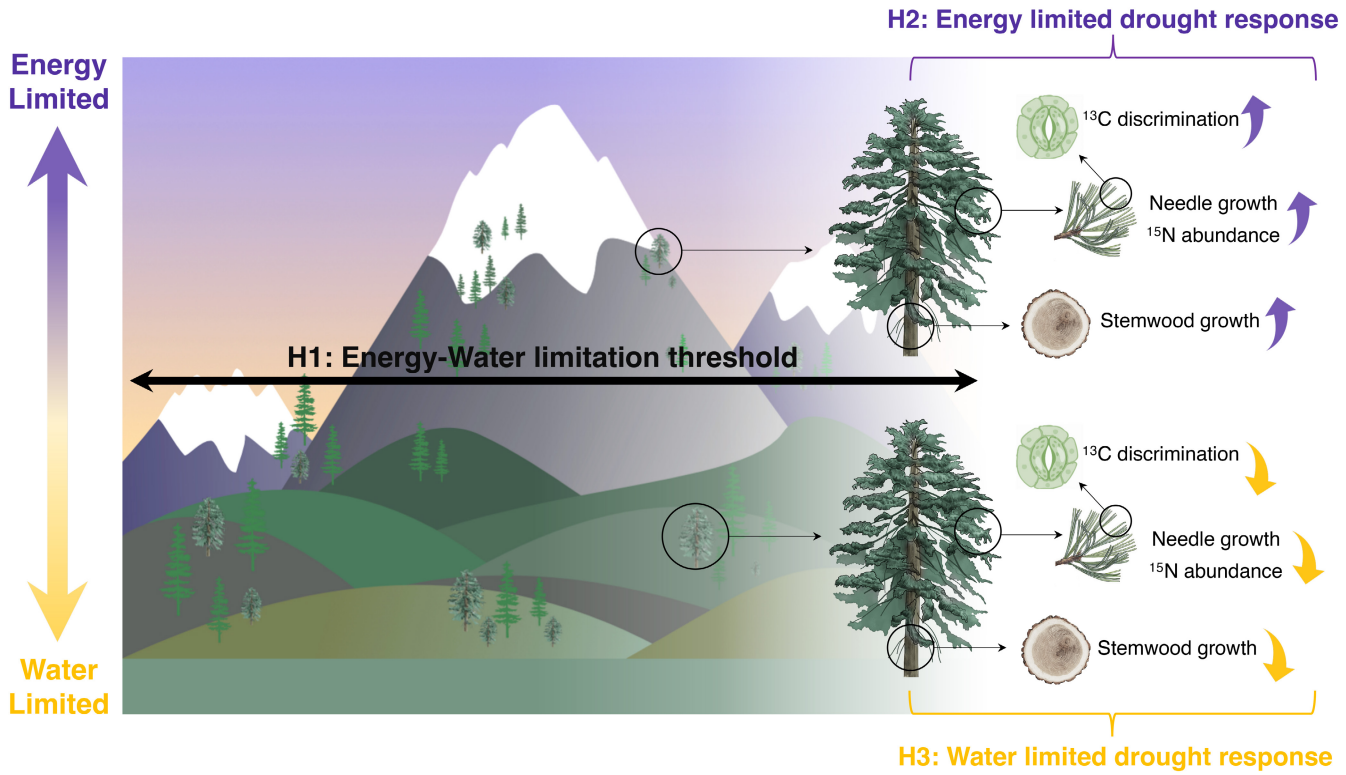

FIGURE 1 Hypotheses of divergent, threshold drought responses across energy- and water-limited systems. H1: the estimated location of the E-W limitation threshold across elevation (yellow shading = water limited and purple shading = energy limited). H2–H3: divergent drought responses at the tree level. Specifically, during drought, trees growing in energy-limited systems experience increases in stemwood growth, needle length, foliar ^{15}N abundance, and carbon isotope discrimination (H2; purple arrows). In contrast, trees growing in water-limited regions experience decreases in stemwood growth, needle length, ^{15}N abundance, and carbon isotope discrimination in response to drought (H3; yellow arrows). These divergent drought responses likely represent co-occurring thresholds in source and sink processes that limit tree growth. [Colour figure can be viewed at wileyonlinelibrary.com]

13652486, 2023, 15, Downloaded from https://onlinelibrary.wiley.com/doi/10.1111/gcb.16740 by National Forest Service Library, Wiley Online Library on [03/08/2023]. See the Terms and Conditions (https://onlinelibrary.wiley.com/terms-and-conditions) on Wiley Online Library for rules of use; OA articles are governed by the applicable Creative Commons License

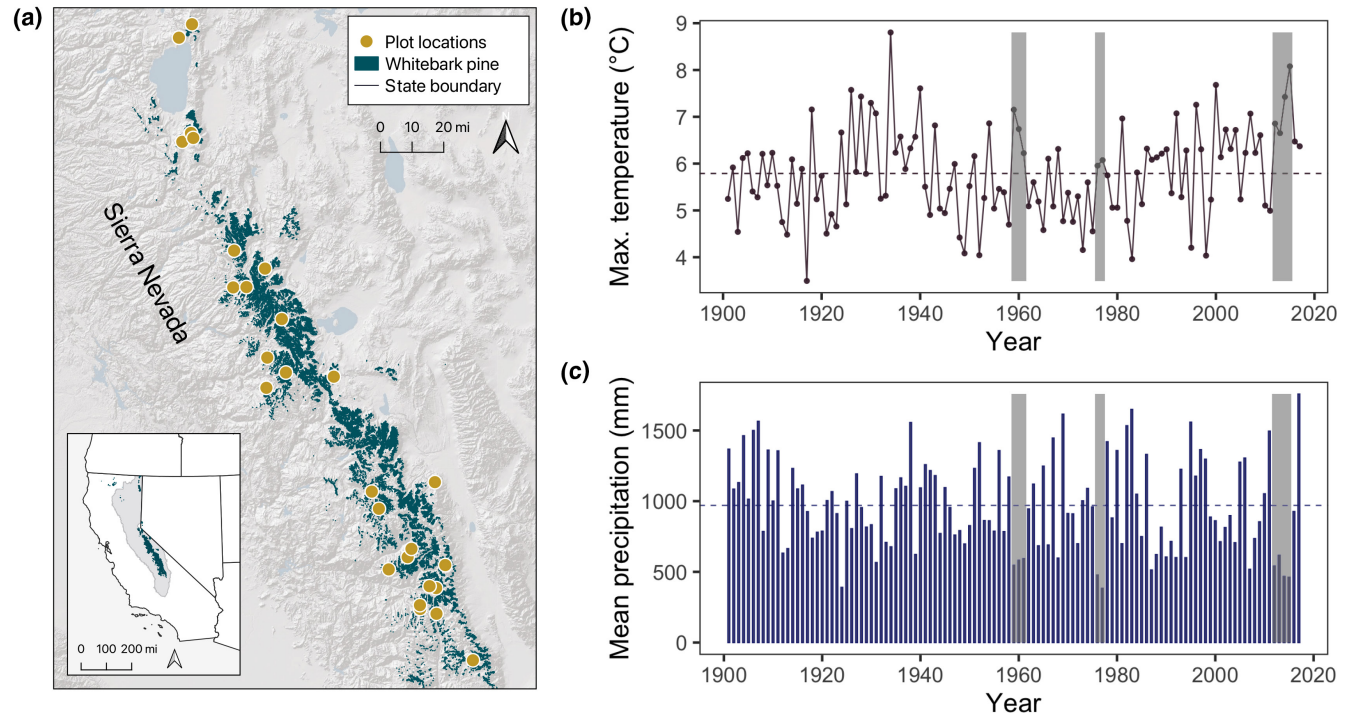

FIGURE 2 (a) Map of the whitebark pine range (green) and study plots (yellow dots) in the Sierra Nevada. Insert shows the whitebark pine range (green) across the Sierra Nevada (grey; USDA Forest Service, 2020). (b, c) Mean annual fall-spring water year maximum temperature and total precipitation (averaged across plots) between 1901 and 2017; dotted horizontal lines delineate mean climate values across all years. Light grey rectangular boxes highlight extreme drought years: 1959–1961, 1976–1977, and 2012–2015. [Colour figure can be viewed at wileyonlinelibrary.com]

2 | METHODS

2.1 | Study site

The Sierra Nevada mountains, which span a large proportion of the eastern edge of California and cross into Nevada around Lake Tahoe (Figure 2), are characterized by a Mediterranean climate, typified by warm, dry summers and cold, wet winters. The mountains span a large elevational gradient, from 300 m in the foothills to the tallest peak in the continental United States (Mt. Whitney: 4421 m; USFS, 2021). This elevation gradient leads to highly variable climatic and vegetation classes (Stephenson, 1988). For example, precipitation ranges from 500 to 2030 mm, falling mostly as snow above 1800 m. Mean annual temperatures range from 5.5 to 15.5°C, corresponding to a growing season range from 94 to 230 days (Millar et al., 2020).

Across the Sierra Nevada's climatic gradient, a number of forest types emerge, starting with oak woodland and mixed conifer forests at low elevations, which transition into montane and upper montane at mid elevations (typically considered more water limited) and finally the subalpine forests at high elevations (considered more energy limited; Stephenson, 1988). The subalpine forests occur between 2000 and 3500 m, and trees range in stature from tall vertical stems at lower elevations to shrub-like *krummholz* growth forms near treeline (Fites-Kaufman et al., 2007). The subalpine forests are comprised primarily of whitebark pine (*P. albicaulis*), lodgepole pine (*Pinus contorta* Dougl.), foxtail pine (*Pinus balfouriana* Grev. & Balf.), limber pine (*Pinus flexilis* James), and mountain hemlock (*Tsuga mertensiana* (Bong.) Carr.; Fites-Kaufman et al., 2007). To reduce potential confounding of species-level physiological differences in traits associated with tolerance of water deficit, we focused on the whitebark pine climatic niche, a tree species that often forms dominant stands in the subalpine primarily between 2100 and 3700 m.

2.2 | Study design

The main objective of the plot selection was to capture the full variation of climate conditions during the extreme drought that occurred between 2012 and 2015 and decouple precipitation and temperature from elevation, thereby increasing the likelihood of capturing the energy–water (E–W) limitation threshold. For the plot selection, we used mean minimum temperature and average snowpack from the Basin Characterization Model (BCMv8; Flint et al., 2021) during the drought years and clipped these maps to the whitebark pine range map of the Sierra Nevada using ArcGIS® (Figure 2a). BCM products use PRISM data (PRISM, Daly et al., 2008), which are downscaled to 270 m, and provide monthly temperature, precipitation, among other variables (Flint et al., 2021).

To select plots, we averaged climate variables between 2012 and 2015 and identified regions of the whitebark pine range that experienced ±1 SD above or below mean snowpack and minimum temperatures, as well as average conditions. In total, five climatic zones were identified and replicated three to five times in different regions of the Sierra Nevada for a total of 27 plots: (1) high snow,

13652486, 2023, 15, Downloaded from https://onlinelibrary.wiley.com/doi/10.1111/gcb.16740 by National Forest Service Library, Wiley Online Library on [03/08/2023]. See the Terms and Conditions (https://onlinelibrary.wiley.com/terms-and-conditions) on Wiley Online Library for rules of use; OA articles are governed by the applicable Creative Commons License

high temperature, (2) low snow, high temperature, (3) low snow, low temperature, (4) high snow, low temperature, and (5) mean snow, mean temperature. This design enabled us to capture both the gradient of snowpack and temperature conditions and largely decouple precipitation from elevation (and to a lesser degree, temperature; Figure S1).

Given the sampling effort and crew costs in remote regions, climatic categories that fell within 2 km of known U.S. Forest Service and National Parks Service monitoring plots were selected to better ensure presence of whitebark pine and sampling success. Three to four polygons were drawn in ArcGIS starting from the closest suitable region to a monitoring plot that included south facing aspects (135°–225°) and avoided slopes too dangerous for sampling (>35°). Ultimately, the plots spanned the northern shore of Lake Tahoe basin to Sequoia National Park in the south (Figure 2). Mean maximum temperature and total precipitation across all plots (calculated between October 1 and June 30; see subsection "Climate data") for the study period was 5.79°C with a range of 0.57–16.26°C and 964.29 mm with a range of 75.75–2837.34 mm, respectively. Mean maximum temperature (January 1–December 31) across all plots was 8.63°C (0.94–18.5°C) and mean total precipitation was 1008.14 mm (11.57–2913.61 mm). For more details on the sampling methodology, please see van Mantgem et al. (in review).

2.3 | Field sampling

This research was conducted on unceded land of many Native American groups. Between 2018 and 2019, crews navigated to polygons in numerical order and selected the first suitable site. The crews selected the site for sampling if >30 whitebark stems were present, the environmental conditions were safe, and if the majority of the stand grew vertically (i.e., avoiding shrubby growth like *krummholz* to reduce bias in comparisons across the Sierra-wide population; Millar et al., 2020). Starting from a randomly selected point within each polygon, crews placed a transect perpendicular to the slope to ensure a similar aspect and elevation. Crews sampled healthy trees along the transect until a minimum of 25 (the target number was 30) stems were sampled; a plot included all trees sampled at the site. If stems were clumped, we sampled one stem per clump. For some plots, all healthy trees were sampled reflecting the variation in tree density across the whitebark pine population in the Sierra Nevada. Healthy stems were defined as trees free of signs and symptoms of biotic agents or severe damage. Crews recorded the GPS location of the start of the transect, and in plots where vertical stems were sparse, crews measured individual stem locations with GPS. One core per stem was extracted at DBH (diameter at breast height, 1.37 m), and a total of 800 tree cores were extracted in the field.

Following protocols outlined by Dudney et al. (2021), healthy needles were extracted from three south-facing, low-lying branches on the first 7–12 sampled stems. A total of 1398 needles were extracted at branch internodes for each year's cohort, and fascicles were present typically between the 2011 and 2017 internodes (internodes were classified by branch nodes). Annual needle length for each tree was estimated from three healthy fascicles selected from each year's needle cohort. The first six of the 12 trees were then selected for stable isotopic analysis, resulting in a total of 1075 stable isotope samples. Due to budget constraints, stable isotope analyses were not conducted for six plots that experienced average climatic conditions relative to the full climate niche. For more sampling details, please refer to Dudney et al. (2021).

2.4 | Climate data and classification of extreme drought years

To model long-term relationships between weather patterns and tree rings using reliable climate records, we used downscaled 4 km resolution PRISM climate data spanning the years 1900–2017 (Figure 2). The weather variables included total annual and monthly precipitation (mm) and mean monthly maximum temperature (°C). PRISM data enabled us to model a longer tree-ring time series versus the more temporally limited BCM dataset, while maintaining consistency across all climate-related analyses. We calculated fall-spring water year temperature and precipitation as mean temperatures and total rainfall that fell between October 1 and June 30 (the weather window that resulted in the most parsimonious model; Table S1). We estimated extreme drought years as follows: first, we identified all years that fell above the mean temperature and below one standard deviation (SD) of the mean precipitation for the study period 1901–2017; second, we classified extreme drought as ≥2 years near or below 1 SD of the mean; third, we ranked these drought events by mean average rainfall and classified the three lowest rainfall drought events as the most extreme (Figure S2). The most extreme droughts were 1976–1977, 2012–2015, and 1959–1961 (Figure 2b,c).

2.5 | Tree rings

Whitebark pine tree cores were prepared following standard protocols outlined by Speer (2010). Specifically, cores were mounted and sanded with increasingly finer grit until ring boundaries were clearly visible. We measured ring widths to the nearest 0.001 mm using WinDENDRO (Regent Instruments Canada Inc.) and a flatbed scanner (2400 dpi). To ensure accuracy, we used a stereo microscope, the Unislide TA tree-ring measuring system (Velmex Inc.), and Measure J2X software (VoorTech Consulting) when rings were too small to measure their widths using the scanner. To achieve high precision in the cross-dating (because whitebark pine tree rings are challenging to cross-date; Millar et al., 2012), we employed a three-stage process: (1) we identified potential marker years for each plot by visually comparing the series within each plot; (2) we cross-dated the series within each plot using the dplR package for R (Bunn, 2010); and (3) we statistically compared our cross-dated series to a whitebark pine chronology developed by Millar et al. (2012). Cross-dated ring width series were double detrended to remove biological growth trends

13652486, 2023, 15, Downloaded from https://onlinelibrary.wiley.com/doi/10.1111/gcb.16740 by National Forest Service Library, Wiley Online Library on [03/08/2023]. See the Terms and Conditions (https://onlinelibrary.wiley.com/terms-and-conditions) on Wiley Online Library for rules of use; OA articles are governed by the applicable Creative Commons License

and minimize the influence of stand dynamics such as disturbance and inter-tree competition (Fritts, 2012). First, each ring width series was divided by a negative exponential curve or linear trend line of negative or zero slope to remove the age-related growth trends. Second, a cubic smoothing spline that preserved 50% of the variance at 67% of the series length was applied to remove residual trends induced by stand dynamics. Through this process, the number of analyzable cores decreased from 800 to 772.

2.6 | Needle length and stable isotopes

To test for variation in stable carbon and nitrogen isotope compositions (carbon: $\delta^{13}C$ and % C and nitrogen: $\delta^{15}N$ and % N) of whitebark pine needles, we first dried the needles (in drying ovens at 60°C), measured needle length (to the nearest mm), and then pulverized 5–10 fascicles in plastic Eppendorf® test tubes using a Bullet Blender (Next Advance, LLC). Test tubes were sent to the UC Davis Analytical Center (Davis, California) where each sample was weighed and encapsulated in tin. Encapsulated samples were then sent to the UC Davis Stable Isotope Facility (Davis, California) and isotope ratios were measured for each sample. Stable isotope ratios and concentrations were estimated using a PDZ Europa Ltd. ANCA-GSL elemental analyzer infracted to a PDZ Europa Ltd. 20–20 continuous flow isotope ratio mass spectrometer (IRMS). Lab reference materials were internally calibrated against international standards including IAEA-600, USGS40, USGS41, USGS-42, USGS-43, USGS-61, USGS-64, and USGS-65. The long-term standard deviation is ±0.2‰ for ^{13}C and ±0.3‰ for ^{15}N.

Carbon and nitrogen isotopic compositions are typically reported in δ notation relative to VPDB (Vienna Pee Dee Belemnite) for carbon and atmospheric N_2 for nitrogen and expressed in per mil (‰), which is equivalent to 10^{-3}. Following Farquhar et al. (1989):

$$\delta^{13}C = \frac{R_{sample}}{R_{standard}} - 1 \quad (1)$$

$$\delta^{15}N = \frac{R_{sample}}{R_{standard}} - 1 \quad (2)$$

where R_{sample} and $R_{standard}$ represent the ratios of $^{13}C/^{12}C$ and $^{15}N/^{14}N$, respectively, for samples and standards. Because $\delta^{13}C$ values were measured across a range of years (2011–2017), they were corrected for rising concentrations of atmospheric CO_2 using annual atmospheric CO_2 data obtained from the La Jolla Pier records (available here: https://scrippsco2.ucsd.edu/data/atmospheric_co2/ljo.html). The data used for our analyses are available on ScienceBase (Dudney et al., 2023).

2.7 | Statistical analyses

To test our hypotheses, we combined long-term tree-ring records (1900–2017) with short-term (2011–2017) needle length and needle stable isotope signatures. The tree-ring records provided long-term measurements that spanned multiple extreme droughts (Figure 2). The short-term needle length and stable isotope measurements provided insight into productivity and photosynthetic capacity during the recent extreme drought in CA (2012–2015). We combined tree rings, stable isotope ratios, and needle length records to test whether these different classes of growth measurements showed consistent or contradictory growth responses during the extreme meteorological drought.

To determine if whitebark pine spanned the E–W limitation threshold, we fitted generalized additive mixed models (GAMMs) using the mgcv package in R, which are well suited for detecting nonlinear relationships (Wood, 2022). We used GAMMs to estimate the shape of the relationship and compared models with and without smoothed terms to determine whether the nonlinear terms reduced model deviance and increased model parsimony. The most parsimonious model (i.e., the model with the lowest AIC) included temperature (°C), precipitation (mm), DBH (cm), and tree height (m) with plot as a random effect (models that included a nested tree-level random effects term were not supported using AIC). The most parsimonious temperature and precipitation variables spanned the fall-spring water year, October 1–June 30 (Table S1). To estimate the temperature and precipitation thresholds, we ran a Monte Carlo simulation, which allowed us to capture the uncertainty of the GAMM coefficients. Specifically, we randomly sampled 10,000 GAMM model coefficients from the variance–covariance matrix. Using these coefficients, we predicted RWI using the ggeffects package (Lüdecke, 2018). Then, we extracted the estimated peak RWI value across temperature and precipitation for each iteration, which allowed us to precisely estimate the mean and 95% CI (confidence interval) of the temperature and precipitation inflection points.

Because outliers were contributing to non-normally distributed residuals, we removed values that were 1.5 times greater than the 75th quantile and 1.5 times less than the 25th quantile. We ensured that our results were consistent with and without outliers. We also found plot random effects effectively controlled for spatial autocorrelation and verified that the detrending analysis controlled for potentially problematic temporal autocorrelation. Finally, we verified that our GAMM results were consistent with generalized linear mixed models (GLMMs) that included quadratic terms (Table S2). Specifically, we fitted GLMMs using the R package lme4 (Bates et al., 2020) with tree growth (RWI) as a function of fall-spring precipitation and temperature, DBH, tree height, and plot random effects. We verified that our GLMM residuals were normally distributed and that temperature and precipitation were not highly correlated ($r < .5$).

We also tested whether the linear relationship between RWI and temperature and precipitation changed direction across temperature quantiles (which would suggest that the system was shifting from energy limited to water limited (Hartl-Meier et al., 2014) and would also corroborate the nonlinear relationships in the GAMMs). Specifically, we estimated six GAMMs with RWI as the response variable and temperature and precipitation as the independent

13652486, 2023, 15, Downloaded from https://onlinelibrary.wiley.com/doi/10.1111/gcb.16740 by National Forest Service Library, Wiley Online Library on [03/08/2023]. See the Terms and Conditions (https://onlinelibrary.wiley.com/terms-and-conditions) on Wiley Online Library for rules of use; OA articles are governed by the applicable Creative Commons License

variables. We included plot random effects and ran these models for each temperature quartile and tercile for a total of six models. We did not include tree as a nested and random effect because it did not improve model fit and caused model singularity; though we verified our results were consistent when using tree nested random effects. Finally, we tested whether the three most extreme droughts (1976–1977, 2012–2015, and 1959–1961) led to similar growth patterns by subtracting the average growth during drought from the mean of the remaining years across temperature terciles and quartiles. To test whether these changes were significant, we used the nonparametric Wilcoxon signed rank tests.

In addition, we tested how the extreme drought between 2012 and 2015 differentially shifted needle length and stable isotope ratios. Because the tree-ring dataset spanned multiple meteorological droughts and provided a substantially longer, more extensive growth record, we expected that the tree-ring models would provide a more precise estimate of the threshold (that corresponded with the transition between energy- and water-limited systems). Therefore, we used the estimated inflection point from the tree-ring records to test whether it was significantly correlated with thresholds in needle length and stable isotope ratios during meteorological drought years (2012–2015). Specifically, we estimated relative change in $\delta^{13}C$, $\delta^{15}N$, and needle length by subtracting meteorological drought years from non-meteorological drought years (2011, 2016–2017) for each tree. Then, we estimated whether the direction of the meteorological drought effect changed above and below the threshold (above the threshold >8.4°C; below the threshold ≤8.4°C) using a GLMM approach with tree-level differences as the response variable, the tree-ring threshold as the explanatory categorical variable (i.e., above or below the threshold), and plot as the random effect (unless random effects reduced model fit).

3 | RESULTS

3.1 | Detecting thresholds in tree growth across temperature and precipitation

GAMM results suggested that RWI was significantly and nonlinearly associated with fall-spring maximum temperature and precipitation (Figure 3; Table 1). These nonlinear relationships were also corroborated using a GLMM with quadratic precipitation and temperature terms (Table S2; Figure S3). The inflection point in the temperature relationship occurred around 8.4°C (95% CI: 7.12; 9.51°C), while the inflection point for precipitation occurred around 1534.0 mm (1194.4; 2243.1 mm). These thresholds were estimated using fall-spring water year variables (October 1–June 30), which were the strongest predictors of growth (Table S1). Furthermore, linear relationships across the temperature gradient corroborated the GAMM estimated nonlinear relationships (Figure 3c,d). In colder regions, RWI was negatively correlated with precipitation and positively correlated with temperature; the direction of these relationships flipped in the warmest regions (Tables S3 and S4).

3.2 | The temperature threshold likely captured the shift from energy- to water-limited tree growth

During extreme meteorological drought, the inflection point in temperature was significantly associated with divergent stemwood growth responses (Estimate: 0.04; $p = .008$; Table S5). Above the inflection point (>8.4°C), extreme meteorological drought was associated with an average decline in RWI (mean and SE: -0.04 ± 0.02). Below the threshold (≤8.4°C), extreme meteorological drought led to an average increase in RWI (0.02 ± 0.006). The relative change in RWI varied by meteorological drought (Figure 4). Surprisingly, the severe 2012–2015 drought did not result in the greatest decline in growth; rather, the 1959–1961 drought resulted in the greatest decline in the warmest regions (Figure 4a,b). Furthermore, during extreme meteorological droughts, the temperatures warmed across all whitebark pine plots, shifting the system in the direction of greater water limitation (Figure 4b), which was associated with higher mean growth in the majority of whitebark pine plots (Figure S4).

In contrast, the precipitation inflection point was not associated with divergent growth responses during meteorological drought. Precipitation levels across all plots did not surpass the estimated precipitation threshold during drought (Figure S5); rather, the precipitation threshold emerged during wetter years, pinpointing the precipitation level where additional precipitation, on average, led to declines in growth (Figure S6). Thus, both extreme dry years and extreme wet years led to declines in growth in specific regions. In drought years, decreased growth was associated with water limitation in warmer regions (Figure 3c,d), whereas in wetter years, decreased growth was likely associated with a shortened growing season due to higher snowpack, particularly in cooler, wetter regions (Figure S7). In summary, divergent stemwood growth responses to extreme meteorological drought corresponded to the temperature threshold, which likely pinpointed where the system transitioned between energy- and water-limited growth (hereafter the E–W limitation threshold; Figure 3a).

3.3 | Co-occurring thresholds in needle growth and stable isotope ratios

During meteorological drought, opposing responses in needle growth and stable isotope ratios corresponded to the stemwood growth temperature threshold (i.e., 8.4°C). For example, needle length increased in colder regions and decreased in the warmest regions during drought (Figure 5a,b), suggesting that water limitation led to declines in needle growth in the warmest regions (Figure 5b). The shift from positive to negative growth responses during drought was significantly correlated with E-W limitation threshold (estimate: 0.71; $p < .001$; Table S5). Below the threshold, meteorological drought led to increases in needle length (mean = 0.54 ± 0.03 cm), while meteorological drought led to declines in needle length (-0.16 ± 0.08 cm) above the threshold.

In addition, greater water limitation during drought was corroborated by changes in $\delta^{13}C$ values, which became less negative

13652486, 2023, 15, Downloaded from https://onlinelibrary.wiley.com/doi/10.1111/gcb.16740 by National Forest Service Library, Wiley Online Library on [03/08/2023]. See the Terms and Conditions (https://onlinelibrary.wiley.com/terms-and-conditions) on Wiley Online Library for rules of use; OA articles are governed by the applicable Creative Commons License

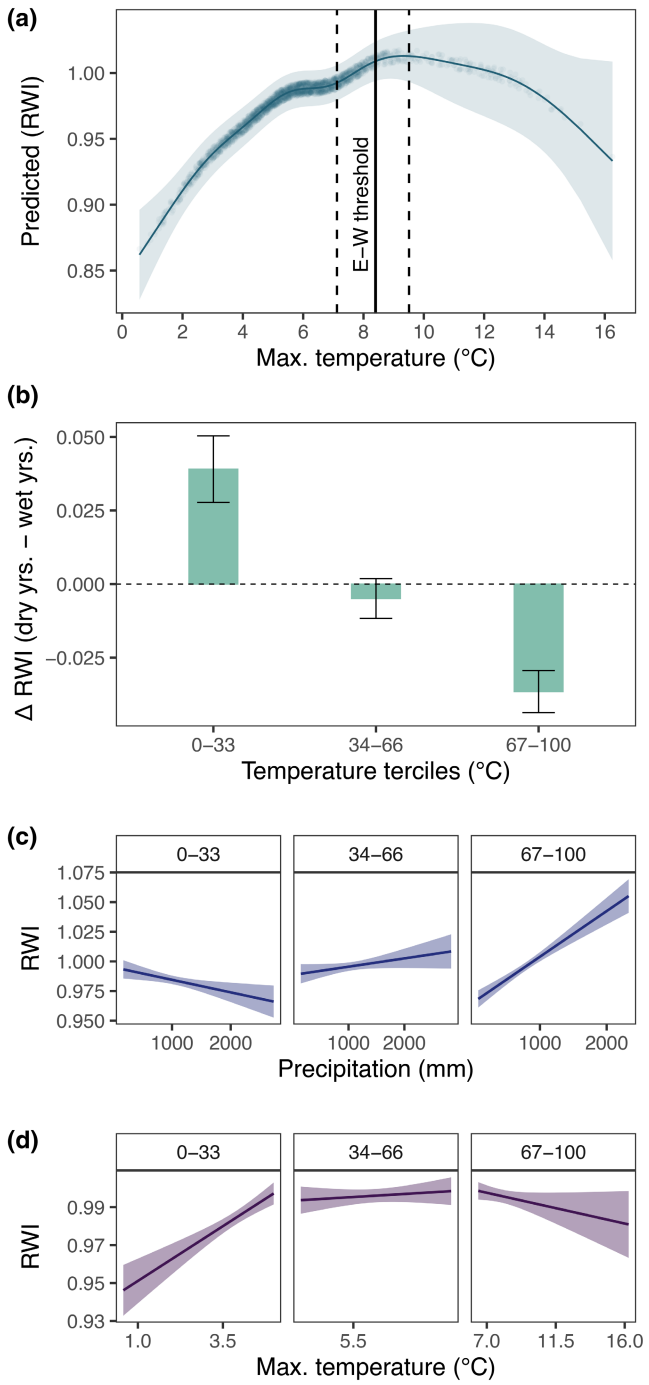

FIGURE 3 The estimated energy–water limitation threshold and corresponding stemwood production relationships across temperature terciles. (a) The marginal effect of temperature on tree-ring index (RWI) between 1900 and 2017. The solid black line and 95% CI black dashed lines illustrate the peak of the nonlinear relationship (i.e., the estimated energy–water limitation threshold); data points are jittered predicted values (height = 0.005) with 95% CI shading. (b) Mean differences in growth between dry years (0–20th percentile range of precipitation) and wet years (21–100th percentile range = wetter conditions); error bars represent one SE of the mean. Relationship between RWI and precipitation (c) and maximum temperature (d) across temperature terciles (0–33rd = 0.57–4.99°C; 34–66th = 5.0–6.44°C; 67–100th = 6.45–16.26°C); shading around linear lines represents the 95% CI. [Colour figure can be viewed at wileyonlinelibrary.com]

TABLE 1 Displaying regression estimates, SEs, and corresponding *p*-values from GAMMs estimating ring width index (RWI).

Parametric coefficients	Estimates	SE	*p*-value
RWI GAMM			
(Intercept)	0.9928	0.0056	**<.001**
DBH (cm)	0.0042	0.0018	**.0168**
Height (m)	−0.0011	0.0020	.5802
Smooth terms	**EDF**	***F*-value**	***p***
s(Precipitation)	2.939	12.552	**<.001**
s(Temperature)	7.147	21.753	**<.001**
s(Plot)	24.702	4.981	**<.001**
N_{plot}	27		
Observations	72,582		
Deviance explained	0.335%		

Note: Bolding represents significant *p*-values ($p < .05$).

(Figure 5c,d) in warmer regions. In contrast, the persistence of energy limitation, even during drought, was corroborated by changes in $\delta^{13}C$ values, which became more negative in colder regions (Figure 5c,d). These divergent responses were significantly correlated with the stemwood growth temperature threshold (Estimate: −0.58; $p = .009$; Table S5). Specifically, below the threshold, $\delta^{13}C$ values became more negative during meteorological drought (−0.39 ± 0.03‰), but increased (became less negative) above the threshold in the warmest regions (0.19 ± 0.09‰; Figure 5c,d).

The stemwood growth temperature threshold was also significantly correlated with differential changes in $\delta^{15}N$ during meteorological drought (Estimate: −0.15; $p = .013$; Table S5). Above the threshold, $\delta^{15}N$ increased (0.13 ± 0.09‰), but below the threshold, $\delta^{15}N$ ratios remained relatively unresponsive to meteorological drought (Figure 5e,f). Thus, the divergent responses in needle length, $\delta^{13}C$, and $\delta^{15}N$ during meteorological drought indicated that the sampled whitebark pine system shifted from primarily energy limited at higher elevation to primarily water limited at lower elevation. This transition likely occurred between 7.12 and 9.51°C and was associated with multiple physiological thresholds which emerged during extreme meteorological drought (Figure 5).

4 | DISCUSSION

Long-term growth patterns in whitebark pine suggested that whitebark pine-dominated forests in the Sierra Nevada spanned both energy- and water-limited systems. The transition between these ecohydrological classes likely promoted the stemwood growth temperature threshold (8.4°C [7.12; 9.51°C]), which corresponded to the E–W limitation threshold. Our sampling design enabled us to

13652486, 2023, 15, Downloaded from https://onlinelibrary.wiley.com/doi/10.1111/gcb.16740 by National Forest Service Library, Wiley Online Library on [03/08/2023]. See the Terms and Conditions (https://onlinelibrary.wiley.com/terms-and-conditions) on Wiley Online Library for rules of use; OA articles are governed by the applicable Creative Commons License

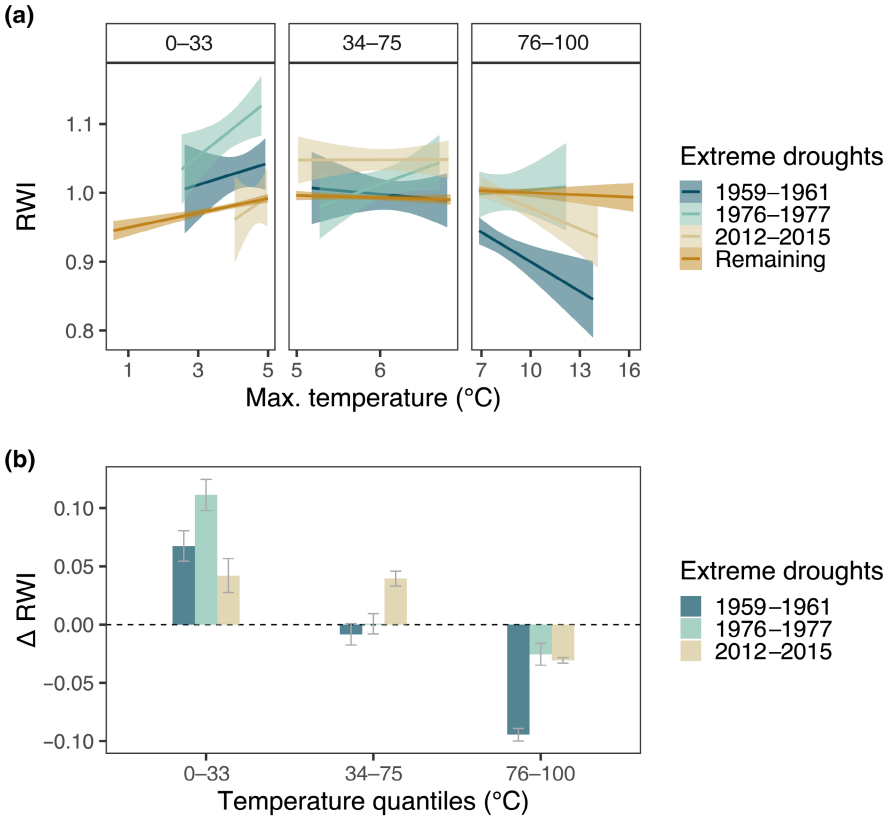

FIGURE 4 Differences in tree growth during the three most extreme droughts. (a) Shifts in RWI during droughts versus the remaining years. Linear lines estimated within temperature quantiles and shading represents the 95% CI around the estimated linear relationship. (b) Mean differences between extreme drought years and the remaining years across the temperature quantiles for the three most extreme droughts, displaying SE bars. [Colour figure can be viewed at wileyonlinelibrary.com]

disentangle climate from elevation and suggested that temperature, not precipitation, was the strongest determinant of whether this system was more energy or water limited (Roebroek et al., 2020). Though temperature mediated the ecohydrological transition in this system, different climatic factors likely drive transitions among other ecohydrological classes that emerge across larger spatial scales (Babst et al., 2019; Gantois, 2022; Roebroek et al., 2020). Interestingly, water limitation still occurred in energy-limited regions—precipitation was positively correlated with whitebark pine growth until reaching the precipitation threshold (Figure S6). Low temperature, however, reduces the length of the growing season, which is likely the strongest control on growth (Bourgouin, 2000; Hartl-Meier et al., 2014; Reich, Luo, et al., 2014). Under forecasted climate warming, whitebark pine growth in energy-limited regions may continue to increase. The corresponding growth declines, however, in water-limited regions (Figure 4; Figure S8) threaten the long-term sustainability of the recently listed whitebark pine species in the Sierra Nevada (U.S. Fish & Wildlife Service, 2022).

Consistent with our hypotheses, the E–W limitation threshold was significantly correlated with threshold responses in needle length and carbon isotope ratios that emerged during extreme meteorological drought (Figure 5; Table S5). These co-occurring thresholds likely captured the shift between energy- and water-limited controls on carbon assimilation. For example, shifts in needle length and $\delta^{13}C$ above the threshold were consistent with drought responses in water-limited conifer forests—declines in water availability are often associated with higher $\delta^{13}C$, shorter needles, (Adams et al., 2015, Dudney et al., 2021), and reduced radial growth (Allen et al., 2015; Zald et al., 2022). In contrast, shifts in needle length and $\delta^{13}C$ below the threshold were consistent with energy-limited responses to declines in precipitation, which can lead to increased gas exchange and leaf productivity (Delucia, 1986; Hultine & Marshall, 2000; Reich, 2014; Reich, Rich, et al., 2014; Shestakova et al., 2017). In addition, during non-drought years, $\delta^{13}C$ values were highest in the coldest regions, which is consistent with temperature–$\delta^{13}C$ relationships found in previous studies (Marshall & Zhang, 1993; McDowell et al., 2010). During meteorological drought, however, $\delta^{13}C$ values increased in warmer regions, reflecting the $\delta^{13}C$ values in colder regions (Figure 5c), suggesting that both high energy and high water limitation lead to similar stable carbon isotope signatures at the species level.

In addition, co-occurring thresholds in source and sink processes that limit tree growth are consistent with theory and previous studies demonstrating that thresholds in higher-level ecosystem attributes can be coupled with thresholds in lower-order ecosystem attributes (Berdugo et al., 2020; Rocha et al., 2018). The co-occurring thresholds appeared to influence stemwood growth in a similar direction, which could indicate multiplicative effects (Rocha et al., 2018), particularly for needle length and carbon isotope ratios (Grossiord et al., 2020). In contrast, during drought, foliar $\delta^{15}N$ increased above the threshold while stemwood and foliar growth declined (Figure 5; Table S5), suggesting that nitrogen cycling processes may be somewhat decoupled from short-term shifts in photosynthesis and growth (Robinson, 2001). Future research testing whether these correlated thresholds are independent (i.e., more strongly coupled with climate) or interconnected (indicating cascading effects on

13652486, 2023, 15, Downloaded from https://onlinelibrary.wiley.com/doi/10.1111/gcb.16740 by National Forest Service Library, Wiley Online Library on [03/08/2023]. See the Terms and Conditions (https://onlinelibrary.wiley.com/terms-and-conditions) on Wiley Online Library for rules of use; OA articles are governed by the applicable Creative Commons License

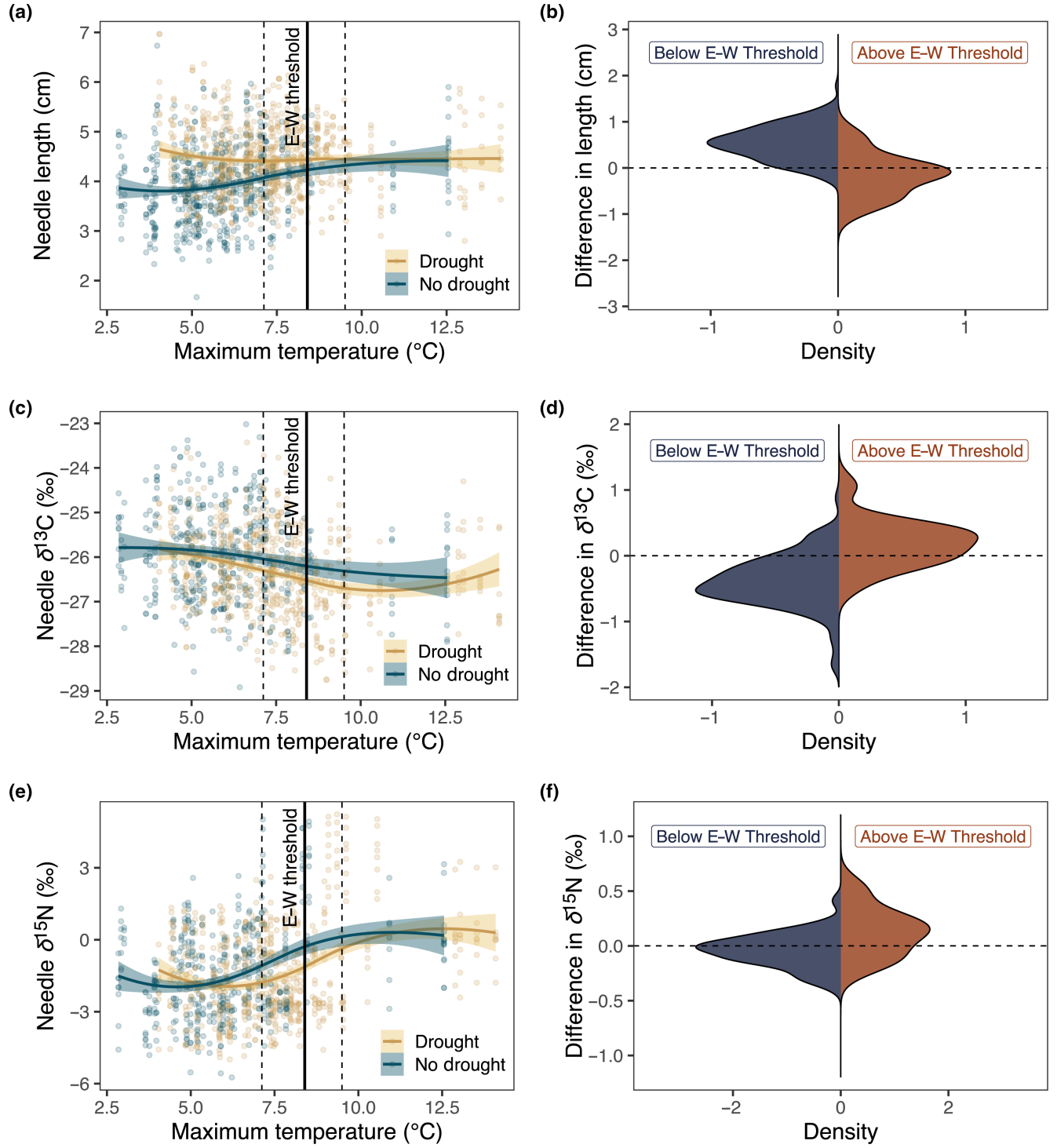

FIGURE 5 Impacts of the 2012–2015 drought on whitebark pine needle growth and stable isotope ratios. Changes in needle length (a), $\delta^{13}C$ (c), and $\delta^{15}N$ (e) during drought years (2012–2015; dark yellow) and non-drought years (2011, 2016–2017; green) across mean, plot-level maximum temperature. The solid, black vertical lines show the estimated E–W threshold and black dashed lines represent the 95% CI. The green and yellow shading around the loess (locally estimated scatterplot smoothing) lines represents the 95% CI. Density figures show differences in needle length (b), $\delta^{13}C$ (d), and $\delta^{15}N$ (f) during drought (mean drought–mean non-drought years; estimated at the tree level) above and below the E–W threshold (8.4°C). [Colour figure can be viewed at wileyonlinelibrary.com]

tree growth) may help clarify the mechanisms of stemwood growth (Cabon et al., 2020; Grossiord et al., 2020; McDowell et al., 2022) and explain why source and sink processes can appear loosely coupled at certain spatial scales (Cabon et al., 2022; Muller et al., 2011).

Although patterns of foliar $\delta^{15}N$ are often highly variable and difficult to interpret (Robinson, 2001), our study suggests that the transition between energy- and water-limited controls on nitrogen cycling helps explain global patterns of foliar $\delta^{15}N$. For example,

13652486, 2023, 15, Downloaded from https://onlinelibrary.wiley.com/doi/10.1111/gcb.16740 by National Forest Service Library, Wiley Online Library on [03/08/2023]. See the Terms and Conditions (https://onlinelibrary.wiley.com/terms-and-conditions) on Wiley Online Library for rules of use; OA articles are governed by the applicable Creative Commons License

even during an extreme drought, foliar $\delta^{15}N$ was surprisingly unresponsive to changes in water availability and temperature below the E–W limitation threshold (i.e., in energy-limited regions). This is consistent with previous studies suggesting that in very cold regions, $\delta^{15}N$ is the least responsive to changes in temperature (Craine et al., 2009). In energy-limited regions, plants are likely more dependent on ectomycorrhizal fungi for macronutrients bound in organic materials, as these fungi often possess saprotrophic capabilities (Hobbie et al., 2000; Steidinger et al., 2019). Whitebark pine, for example, often forms relationships with ectomycorrhizal fungi (Cripps & Antibus, 2011), which supply ^{15}N-depleted nitrogen (Hobbie & Colpaert, 2003). Our results suggest energy-limited forests may be associated with high mycorrhizal dependence for N, as average foliar $\delta^{15}N$ values were negative but became more positive in water-limited regions (Figure 5). Less negative foliar $\delta^{15}N$ values above the E–W threshold are consistent with a global study that measured an average shift from negative to positive foliar $\delta^{15}N$ within a similar temperature range (Craine et al., 2009). Thus, the transition from primarily energy- to water-limited systems likely corresponds to increases in nitrogen availability—due to higher rates of decomposition in water-limited regions (Tuomi et al., 2009)—which may reduce the dependence on mycorrhizae for organically bound nitrogen.

Opposing drought responses across the E–W threshold are consistent with previous studies in montane regions, including Switzerland (Sturm et al., 2022), Italy (Lewińska et al., 2018), and Canada (Kljun et al., 2006). These studies also showed that as the drought extended beyond the first year, productivity declined. Similarly, though whitebark pine continued to experience average-to-above average stem and needle growth during the drought, growth trends declined across drought years (Figure S9), corroborating previous work suggesting that energy-limited growth is decreasing in a warming world (Babst et al., 2019). Furthermore, subalpine systems occur within a broad range of precipitation and temperature gradients (Arekhi et al., 2018; Danby, 2011; Millar & Rundel, 2016), suggesting the spatial extent of energy limitation on growth varies by mountain range. In California's White Mountains, for example, which are drier than the Sierra Nevada, only trees growing within 60–80 m of treeline were positively correlated with temperature (Salzer et al., 2014). In addition, a recent study suggested that tree growth-temperature inflection points vary dramatically within the United States (i.e., ranging between 10°C and 30°C; Gantois, 2022). Species traits, as well as other ecohydrological classes, may be leading to highly variable temperature inflection points across large geographic gradients (Roebroek et al., 2020). There may also be genetic differences as a result of adaptation that mediate threshold responses; recent results from a whitebark pine study in the Sierra Nevada found stemwood growth during drought was linked to genotypic variation in climate-associated loci (van Mantgem et al. in review).

Finally, the E–W limitation threshold could influence mechanisms that confer biotic agent resistance in trees and future vulnerability under warming and drought. Whitebark pine growing in highly energy-limited regions historically experienced low rates of biotic attack from pest and pathogens (Dudney et al., 2020; Millar et al., 2012). As a consequence, resistance mechanisms, including growth-defense trade-offs and resin production (Anderegg et al., 2015; Herms & Mattson, 1992; Valor et al., 2021), may vary across the E–W limitation threshold. Historically, low rates of biotic attack (also constrained by low temperatures (Bentz et al., 2010, Dudney et al., 2020)) in energy-limited systems may have led to lower adaptive potential, which could be related to the high rates of mortality in whitebark pine throughout its range (Goeking & Izlar, 2018). Furthermore, the E–W threshold may lead to differences in whitebark pine's vulnerability to pathogen infection. For example, the pathogen, *Cronartium ribicola*, infects through needle stomata (Hunt et al., 2007); therefore, the timing and duration of gas exchange during drought may lead to increased infection vulnerability in energy-limited regions and decreased vulnerability in water-limited regions (Dudney et al., 2021). The transition between energy- and water-limited regions not only promotes co-occurring thresholds in source and sink processes that limit tree growth, but also likely contributes to divergent patterns of tree vulnerability to pest and pathogen outbreaks.

5 | CONCLUSION

Ecohydrological classes and the transitions between them provide critical insight into the global vulnerability of forests to climate change (Brodribb et al., 2020). Shifts in the dominant climatic controls on whitebark pine growth likely promoted multiple, co-occurring thresholds in tree growth, as well as carbon and nutrient cycling. Disentangling whether these co-occurring thresholds are independent or cascading will provide important insight into the mechanisms driving climate change-induced shifts in forest productivity. Furthermore, thresholds likely occur globally among ecohydrological classes (e.g., energy limited, water limited, precipitation driven, rooting space limited, etc.; see Roebroek et al., 2020), potentially leading to unexpected meteorological drought responses in various vegetation types. Not only does the transition between ecohydrological class likely promote divergent growth responses during drought, long-term adaptations to the dominant climatic controls may lead to contrasting probabilities of pest and pathogen outbreaks (Stephenson et al., 2019; Wong & Daniels, 2017). Thus, predictions of drought impacts on forest productivity under climate change will be greatly improved by including interactions with ecohydrological classes.

AUTHOR CONTRIBUTIONS

Author contributions are defined using the Contributor Roles Taxonomy (CRediT; https://casrai.org/credit/). Conceptualization: J.D.; data curation: P.vM., J.D., J.C.B.N.; formal analysis: J.D., A.M.L.; funding: J.D., P.vM., J.C.B.N.; methodology: J.D., J.C.B.N., C.E.W., A.M.L.; project administration: P.vM., J.D., J.C.B.N; supervision: J.C.B.N., J.D.; tree core preparation, reading, and plot chronologies:

13652486, 2023, 15, Downloaded from https://onlinelibrary.wiley.com/doi/10.1111/gcb.16740 by National Forest Service Library, Wiley Online Library on [03/08/2023]. See the Terms and Conditions (https://onlinelibrary.wiley.com/terms-and-conditions) on Wiley Online Library for rules of use; OA articles are governed by the applicable Creative Commons License

H.Z.; stable isotope preparation: J.C.B.N.; J.D., J.C., A.M.L.; visualization: J.D., A.M.L.; writing—original draft: J.D; writing—review and editing: A.M.L., P.vM., C.E.W., H.Z., J.C., J.C.B.N., and E.M.

ACKNOWLEDGMENTS

We thank our crew lead, Sean Auclair, and crew members, Rosa Cox, Sam Zuckerman, as well as Anne Pfaff and Michéle Slaton for assistance in organizing field work. BCM climate data were provided by Lori and Alan Flint. We thank Connie Millar for help with whitebark pine chronologies and plot selection. Funding was provided by the U.S. Fish and Wildlife Service, the U.S. Geological Survey's Ecosystems Mission Area, and the National Park Service Inventory and Monitoring Program. We thank Amy Vandergast for project support and Alexandra Atlee Phillips and Zuzanna Drozdz for Figure 1 image and design contributions. Dudney acknowledges support from the National Science Foundation, the Wilderness Society, and the David H. Smith Conservation Research Fellowship. Latimer acknowledges support under Hatch Project CA-D-PLS-2017-H. Any use of trade, firm, or product names is for descriptive purposes only and does not imply endorsement by the U.S. Government.

CONFLICT OF INTEREST STATEMENT

The authors declare no competing interests.

DATA AVAILABILITY STATEMENT

Data and code are available at https://github.com/WildEcology/EW_threshold, Sciencebase, and OSF: 10.17605/OSF.IO/CVZNH

ORCID

Joan Dudney https://orcid.org/0000-0003-3986-065X
Claire E. Willing https://orcid.org/0000-0002-7563-242X

REFERENCES

Adams, H. D., Collins, A. D., Briggs, S. P., Vennetier, M., Dickman, L. T., Sevanto, S. A., Garcia-Forner, N., Powers, H. H., & McDowell, N. G. (2015). Experimental drought and heat can delay phenological development and reduce foliar and shoot growth in semiarid trees. *Global Change Biology*, *21*, 4210–4220.

Allen, C. D., Breshears, D. D., & McDowel, N. G. (2015). On underestimation of global vulnerability to tree mortality and forest die-off from hotter drought in the Anthropocene. *Ecosphere*, *6*, 1–55.

Allen, C. D., Macalady, A. K., Chenchouni, H., Bachelet, D., McDowell, N., Vennetier, M., Kitzberger, T., Rigling, A., Breshears, D. D., (Ted) Hogg, E. H., Gonzalez, P., Fensham, R., Zhang, Z., Castro, J., Demidova, N., Lim, J.-H., Allard, G., Running, S. W., Semerci, A., & Cobb, N. (2010). A global overview of drought and heat-induced tree mortality reveals emerging climate change risks for forests. *Forest Ecology and Management*, *259*, 660–684.

Amundson, R., Austin, A. T., Schuur, E. A. G., Yoo, K., Matzek, V., Kendall, C., Uebersax, A., Brenner, D., & Baisden, W. T. (2003). Global patterns of the isotopic composition of soil and plant nitrogen. *Global Biogeochemical Cycles*, *17*, 1031–1035.

Anderegg, W. R. L., Hicke, J. A., Fisher, R. A., Allen, C. D., Aukema, J., Bentz, B., Hood, S., Lichstein, J. W., Macalady, A. K., McDowell, N., Pan, Y., Raffa, K., Sala, A., Shaw, J. D., Stephenson, N. L., Tague, C., & Zeppel, M. (2015). Tree mortality from drought, insects, and their interactions in a changing climate. *New Phytologist*, *208*, 674–683.

Anderegg, W. R. L., Trugman, A. T., Badgley, G., Anderson, C. M., Bartuska, A., Ciais, P., Cullenward, D., Field, C. B., Freeman, J., Goetz, S. J., Hicke, J. A., Huntzinger, D., Jackson, R. B., Nickerson, J., Pacala, S., & Randerson, J. T. (2020). Climate-driven risks to the climate mitigation potential of forests. *Science*, *368*, 891–901.

Arekhi, M., Yesil, A., Ozkan, U. Y., & Balik Sanli, F. (2018). Detecting treeline dynamics in response to climate warming using forest stand maps and Landsat data in a temperate forest. *Forest Ecosystems*, *5*, 23.

Auyeung, D. S. N., Suseela, V., & Dukes, J. S. (2013). Warming and drought reduce temperature sensitivity of nitrogen transformations. *Global Change Biology*, *19*, 662–676.

Babst, F., Bouriaud, O., Poulter, B., Trouet, V., Girardin, M. P., & Frank, D. C. (2019). Twentieth century redistribution in climatic drivers of global tree growth. *Science Advances*, *5*, eaat4313.

Bates, D., Maechler, M., Bolker, B., Walker, S., Christensen, R. H. B., Singmann, H., Dai, B., Scheipl, F., Grothendieck, G., Green, P., & Fox, J. (2020). lme4: Linear Mixed-Effects Models using "Eigen" and S4.

Bentz, B. J., Regniere, J., Fettig, C. J., Hansen, E. M., Hayes, J. L., Hicke, J. A., Kelsey, R. G., Negron, J. F., & Seybold, S. J. (2010). Climate change and bark beetles of the Western United States and Canada: Direct and indirect effects. *Bioscience*, *60*, 602–613.

Berdugo, M., Delgado-Baquerizo, M., Soliveres, S., Hernández-Clemente, R., Zhao, Y., Gaitán, J. J., Gross, N., Saiz, H., Maire, V., Lehmann, A., Rillig, M. C., Solé, R. V., & Maestre, F. T. (2020). Global ecosystem thresholds driven by aridity. *Science*, *367*, 787–790.

Bourgouin, P. (2000). A method to determine precipitation types. *Weather and Forecasting*, *15*, 583–592.

Brodribb, T. J., Powers, J., Cochard, H., & Choat, B. (2020). Hanging by a thread? Forests and drought. *Science*, *368*, 261–266.

Bucholz, E. R., Waring, K. M., Kolb, T. E., Swenson, J. K., & Whipple, A. V. (2020). Water relations and drought response of *Pinus strobiformis*. *Canadian Journal of Forest Research*, *50*, 905–916.

Buckley, T. N. (2005). The control of stomata by water balance. *New Phytologist*, *168*, 275–292.

Bunn, A. G. (2010). Statistical and visual crossdating in R using the dplR library. *Dendrochronologia*, *28*, 251–258.

Cabon, A., Kannenberg, S. A., Arain, A., Babst, F., Baldocchi, D., Belmecheri, S., Delpierre, N., Guerrieri, R., Maxwell, J. T., McKenzie, S., Meinzer, F. C., Moore, D. J. P., Pappas, C., Rocha, A. V., Szejner, P., Ueyama, M., Ulrich, D., Vincke, C., Voelker, S. L., … Anderegg, W. R. L. (2022). Cross-biome synthesis of source versus sink limits to tree growth. *Science*, *376*, 758–761.

Cabon, A., Peters, R. L., Fonti, P., Martínez-Vilalta, J., & De Cáceres, M. (2020). Temperature and water potential co-limit stem cambial activity along a steep elevational gradient. *New Phytologist*, *226*, 1325–1340.

Cook, B. I., Mankin, J. S., & Anchukaitis, K. J. (2018). Climate change and drought: From past to future. *Current Climate Change Reports*, *4*, 164–179.

Craine, J. M., Elmore, A. J., Aidar, M. P. M., Bustamante, M., Dawson, T. E., Hobbie, E. A., Kahmen, A., Mack, M. C., McLauchlan, K. K., Michelsen, A., Nardoto, G. B., Pardo, L. H., Peñuelas, J., Reich, P. B., Schuur, E. A. G., Stock, W. D., Templer, P. H., Virginia, R. A., Welker, J. M., & Wright, I. J. (2009). Global patterns of foliar nitrogen isotopes and their relationships with climate, mycorrhizal fungi, foliar nutrient concentrations, and nitrogen availability. *New Phytologist*, *183*, 980–992.

Cripps, C. L., Antibus, R. K. (2011). Native ectomycorrhizal fungi of limber and whitebark pine: Necessary for forest sustainability In R. E. Keane, D. F. Tomback, M. P. Murray, & C. M. Smith (Eds.), *The future of high-elevation, five-needle white pines in Western North America: proceedings of the High Five Symposium (RMRS-P-63)*, Missoula MT, 28–30 June 2010 (pp. 37–44). Department of Agriculture, Forest Service, Rocky Mountain Research Station.

13652486, 2023, 15, Downloaded from https://onlinelibrary.wiley.com/doi/10.1111/gcb.16740 by National Forest Service Library, Wiley Online Library on [03/08/2023]. See the Terms and Conditions (https://onlinelibrary.wiley.com/terms-and-conditions) on Wiley Online Library for rules of use; OA articles are governed by the applicable Creative Commons License

Daly, C., Halbleib, M., Smith, J. I., Gibson, W. P., Doggett, M. K., Taylor, G. H., Curtis, J., & Pasteris, P. P. (2008). Physiographically sensitive mapping of climatological temperature and precipitation across the conterminous United States. *International Journal of Climatology*, *28*, 2031–2064.

Danby, R. K. (2011). Monitoring Forest-tundra ecotones at multiple scales. *Geography Compass*, *5*, 623–640.

Day, T. A., DeLucia, E. H., & Smith, W. K. (1989). Influence of cold soil and snowcover on photosynthesis and leaf conductance in two Rocky Mountain conifers. *Oecologia*, *80*, 546–552.

Day, T. A., Heckathorn, S. A., & DeLucia, E. H. (1991). Limitations of photosynthesis in *Pinus taeda* L. (Loblolly Pine) at low soil temperatures 1. *Plant Physiology*, *96*, 1246–1254.

Delucia, E. H. (1986). Effect of low root temperature on net photosynthesis, stomatal conductance and carbohydrate concentration in Engelmann spruce (*Picea engelmannii* Parry ex Engelm.) seedlings. *Tree Physiology*, *2*, 143–154.

Dobbertin, M., Eilmann, B., Bleuler, P., Giuggiola, A., Graf Pannatier, E., Landolt, W., Schleppi, P., & Rigling, A. (2010). Effect of irrigation on needle morphology, shoot and stem growth in a drought-exposed *Pinus sylvestris* forest. *Tree Physiology*, *30*, 346–360.

Dudney, J., Latimer, A., van Mantgem, P., Zald, H., Willing, C., Nesmith, J. C. B., Cribbs, J., & Milano, E. (2023). Energy-water limitation threshold in whitebark pine. https://www.sciencebase.gov/catalog/item/

Dudney, J., Nesmith, J. C. B., Cahill, M. C., Cribbs, J. E., Duriscoe, D. M., Das, A. J., Stephenson, N. L., & Battles, J. J. (2020). Compounding effects of white pine blister rust, mountain pine beetle, and fire threaten four white pine species. *Ecosphere*, *11*, e03263.

Dudney, J., Willing, C. E., Das, A. J., Latimer, A. M., Nesmith, J. C. B., & Battles, J. J. (2021). Nonlinear shifts in infectious rust disease due to climate change. *Nature Communications*, *12*, 5102.

Farquhar, G. D., Ehleringer, J. R., & Hubick, K. T. (1989). Carbon isotope discrimination and photosynthesis. *Annual Review of Plant Physiology and Plant Molecular Biology*, *40*, 503–537.

Field, R., O'Brien, E. M., & Whittaker, R. J. (2005). Global models for predicting Woody Plant richness from climate: Development and evaluation. *Ecology*, *86*, 2263–2277.

Fites-Kaufman, J. A., Rundel, P., Stephenson, N., & Weixelman, D. A. (2007). Montane and subalpine vegetation of the Sierra Nevada and Cascade ranges. In M. Barbour, T. Keeler-Wolf, & A. A. Schoenherr (Eds.), *Terrestrial vegetation of California* (3rd ed., pp. 456–501). University of California Press.

Flint, L. E., Flint, A. L., & Stern, M. A. (2021). The basin characterization model—A regional water balance software package. Page 85. Report, Reston, VA.

Fritts, H. (2012). *Tree rings and climate*. Elsevier.

Gantois, J. (2022). New tree-level temperature response curves document sensitivity of tree growth to high temperatures across a US-wide climatic gradient. *Global Change Biology*, *28*, 6002–6020.

Gessler, A., Ferrio, J. P., Hommel, R., Treydte, K., Werner, R. A., & Monson, R. K. (2014). Stable isotopes in tree rings: Towards a mechanistic understanding of isotope fractionation and mixing processes from the leaves to the wood. *Tree Physiology*, *34*, 796–818.

Goeking, S. A., & Izlar, D. K. (2018). Pinus albicaulis Engelm. (Whitebark pine) in mixed-species stands throughout its US range: Broad-scale indicators of extent and recent decline. *Forests*, *9*, 131.

Grossiord, C., Buckley, T. N., Cernusak, L. A., Novick, K. A., Poulter, B., Siegwolf, R. T. W., Sperry, J. S., & McDowell, N. G. (2020). Plant responses to rising vapor pressure deficit. *New Phytologist*, *226*, 1550–1566.

Guérin, M., Martin-Benito, D., von Arx, G., Andreu-Hayles, L., Griffin, K. L., Hamdan, R., McDowell, N. G., Muscarella, R., Pockman, W., & Gentine, P. (2018). Interannual variations in needle and sapwood traits of *Pinus edulis* branches under an experimental drought. *Ecology and Evolution*, *8*, 1655–1672.

Hammond, W. M., Williams, A. P., Abatzoglou, J. T., Adams, H. D., Klein, T., López, R., Sáenz-Romero, C., Hartmann, H., Breshears, D. D., & Allen, C. D. (2022). Global field observations of tree die-off reveal hotter-drought fingerprint for Earth's forests. *Nature Communications*, *13*, 1761.

Handley, L. L., Austin, A. T., Stewart, G. R., Robinson, D., Scrimgeour, C. M., Raven, J. A., Heaton, T. H. E., & Schmidt, S. (1999). The 15N natural abundance (δ15N) of ecosystem samples reflects measures of water availability. *Functional Plant Biology*, *26*, 185–199.

Hartl-Meier, C., Zang, C., Dittmar, C., Esper, J., Göttlein, A., & Rothe, A. (2014). Vulnerability of Norway spruce to climate change in mountain forests of the European Alps. *Climate Research*, *60*, 119–132.

Herms, D. A., & Mattson, W. J. (1992). The dilemma of plants: To grow or defend. *The Quarterly Review of Biology*, *67*, 283–335.

Hillebrand, H., Donohue, I., Harpole, W. S., Hodapp, D., Kucera, M., Lewandowska, A. M., Merder, J., Montoya, J. M., & Freund, J. A. (2020). Thresholds for ecological responses to global change do not emerge from empirical data. *Nature Ecology & Evolution*, *4*, 1502–1509.

Hobbie, E. A., & Colpaert, J. V. (2003). Nitrogen availability and colonization by mycorrhizal fungi correlate with nitrogen isotope patterns in plants. *New Phytologist*, *157*, 115–126.

Hobbie, S. E., Schimel, J. P., Trumbore, S. E., & Randerson, J. R. (2000). Controls over carbon storage and turnover in high-latitude soils. *Global Change Biology*, *6*, 196–210.

Hultine, K. R., & Marshall, J. D. (2000). Altitude trends in conifer leaf morphology and stable carbon isotope composition. *Oecologia*, *123*, 32–40.

Hunt, R. S., Roke, G., & Jensen, G. D. (2007). Initiation of stem infection in western white pine by blister rust [*Cronartium ribicola*]. *Canadian Journal of Plant Pathology*, *29*, 18–24.

Jankowski, A., Wyka, T. P., Żytkowiak, R., Nihlgård, B., Reich, P. B., & Oleksyn, J. (2017). Cold adaptation drives variability in needle structure and anatomy in *Pinus sylvestris* L. along a 1,900 km temperate–boreal transect. *Functional Ecology*, *31*, 2212–2223.

Jenerette, G. D., Barron-Gafford, G. A., Guswa, A. J., McDonnell, J. J., & Villegas, J. C. (2012). Organization of complexity in water limited ecohydrology. *Ecohydrology*, *5*, 184–199.

Jolly, W. M., Dobbertin, M., Zimmermann, N. E., & Reichstein, M. (2005). Divergent vegetation growth responses to the 2003 heat wave in the Swiss Alps. *Geophysical Research Letters*, *32*, L18409.

Kirschbaum, M. U. F. (1995). The temperature dependence of soil organic matter decomposition, and the effect of global warming on soil organic C storage. *Soil Biology and Biochemistry*, *27*, 753–760.

Klein, T. (2014). The variability of stomatal sensitivity to leaf water potential across tree species indicates a continuum between isohydric and anisohydric behaviours. *Functional Ecology*, *28*, 1313–1320.

Kljun, N., Black, T. A., Griffis, T. J., Barr, A. G., Gaumont-Guay, D., Morgenstern, K., McCaughey, J. H., & Nesic, Z. (2006). Response of net ecosystem productivity of three boreal forest stands to drought. *Ecosystems*, *9*, 1128–1144.

Larsen, K. S., Andresen, L. C., Beier, C., Jonasson, S., Albert, K. R., Ambus, P., Arndal, M. F., Carter, M. S., Christensen, S., Holmstrup, M., Ibrom, A., Kongstad, J., Van Der Linden, L., Maraldo, K., Michelsen, A., Mikkelsen, T. N., Pilegaard, K., Priemé, A., Ro-Poulsen, H., … Stevnbak, K. (2011). Reduced N cycling in response to elevated CO_2, warming, and drought in a Danish heathland: Synthesizing results of the CLIMAITE project after two years of treatments. *Global Change Biology*, *17*, 1884–1899.

Lewińska, K. E., Ivits, E., Schardt, M., & Zebisch, M. (2018). Drought impact on phenology and Green biomass production of Alpine Mountain Forest—Case study of South Tyrol 2001–2012 inspected with MODIS time series. *Forests*, *9*, 91.

Lloyd-Hughes, B. (2014). The impracticality of a universal drought definition. *Theoretical and Applied Climatology*, *117*, 607–611.

13652486, 2023, 15, Downloaded from https://onlinelibrary.wiley.com/doi/10.1111/gcb.16740 by National Forest Service Library, Wiley Online Library on [03/08/2023]. See the Terms and Conditions (https://onlinelibrary.wiley.com/terms-and-conditions) on Wiley Online Library for rules of use; OA articles are governed by the applicable Creative Commons License

Lüdecke, D. (2018). Ggeffects: Tidy data frames of marginal effects from regression models. *Journal of Open Source Software*, *3*, 772.
Mahalovich, M. F., Kimsey, M. J., Fortin-Noreus, J. K., & Robbins, C. T. (2016). Isotopic heterogeneity in whitebark pine (*Pinus albicaulis* Engelm.) nuts across geographic, edaphic and climatic gradients in the northern Rockies (USA). *Forest Ecology and Management*, *359*, 174–189.
Marquis, B., Bergeron, Y., Simard, M., & Tremblay, F. (2020). Probability of spring frosts, not growing degree-days, drives onset of spruce bud burst in plantations at the boreal-temperate Forest ecotone. *Frontiers in Plant Science*, *11*, 1031.
Marshall, J. D., & Zhang, J. (1993). 13—altitudinal variation in carbon isotope discrimination by conifers. In J. R. Ehleringer, A. E. Hall, & G. D. Farquhar (Eds.), *Stable isotopes and plant carbon-water relations* (pp. 187–199). Academic Press.
McDowell, N., Pockman, W. T., Allen, C. D., Breshears, D. D., Cobb, N., Kolb, T., Plaut, J., Sperry, J., West, A., Williams, D. G., & Yepez, E. A. (2008). Mechanisms of plant survival and mortality during drought: Why do some plants survive while others succumb to drought? *New Phytologist*, *178*, 719–739.
McDowell, N. G., Allen, C. D., & Marshall, L. (2010). Growth, carbon-isotope discrimination, and drought-associated mortality across a *Pinus ponderosa* elevational transect. *Global Change Biology*, *16*, 399–415.
McDowell, N. G., Sapes, G., Pivovaroff, A., Adams, H. D., Allen, C. D., Anderegg, W. R. L., Arend, M., Breshears, D. D., Brodribb, T., Choat, B., Cochard, H., De Cáceres, M., De Kauwe, M. G., Grossiord, C., Hammond, W. M., Hartmann, H., Hoch, G., Kahmen, A., Klein, T., … Xu, C. (2022). Mechanisms of woody-plant mortality under rising drought, CO_2 and vapour pressure deficit. *Nature Reviews Earth & Environment*:1–15, *3*, 294–308.
Millar, C. I., Delany, D. L., & Westfall, R. D. (2020). From treeline to species line: Thermal patterns and growth relationships across the krummholz zone of whitebark pine, Sierra Nevada, California, USA. *Arctic, Antarctic, and Alpine Research*, *52*, 390–407.
Millar, C. I., & Rundel, P. W. (2016). *TWENTY-EIGHT. Subalpine forests* (pp. 579–612). Ecosystems of California. University of California Press.
Millar, C. I., Westfall, R. D., Delany, D. L., Bokach, M. J., Flint, A. L., & Flint, L. E. (2012). Forest mortality in high-elevation whitebark pine (*Pinus albicaulis*) forests of eastern California, USA: Influence of environmental context, bark beetles, climatic water deficit, and warming. *Canadian Journal of Forest Research*, *42*, 749–765.
Moyes, A. B., Germino, M. J., & Kueppers, L. M. (2015). Moisture rivals temperature in limiting photosynthesis by trees establishing beyond their cold-edge range limit under ambient and warmed conditions. *New Phytologist*, *207*, 1005–1014.
Muller, B., Pantin, F., Génard, M., Turc, O., Freixes, S., Piques, M., & Gibon, Y. (2011). Water deficits uncouple growth from photosynthesis, increase C content, and modify the relationships between C and growth in sink organs. *Journal of Experimental Botany*, *62*, 1715–1729.
Olszyk, D., Wise, C., VanEss, E., Apple, M., & Tingey, D. (1998). Phenology and growth of shoots, needles, and buds of Douglas-fir seedlings with elevated CO_2 and (or) temperature. *Canadian Journal of Botany*, *76*, 1991–2001.
Ordoñez, J. C., Van Bodegom, P. M., Witte, J.-P. M., Wright, I. J., Reich, P. B., & Aerts, R. (2009). A global study of relationships between leaf traits, climate and soil measures of nutrient fertility. *Global Ecology and Biogeography*, *18*, 137–149.
Poorter, H., Niinemets, Ü., Poorter, L., Wright, I. J., & Villar, R. (2009). Causes and consequences of variation in leaf mass per area (LMA): A meta-analysis. *New Phytologist*, *182*, 565–588.
Reich, P. B. (2014). The world-wide 'fast–slow' plant economics spectrum: A traits manifesto. *Journal of Ecology*, *102*, 275–301.
Reich, P. B., Luo, Y., Bradford, J. B., Poorter, H., Perry, C. H., & Oleksyn, J. (2014). Temperature drives global patterns in forest biomass distribution in leaves, stems, and roots. *Proceedings of the National Academy of Sciences of the United States of America*, *111*, 13721–13726.
Reich, P. B., Rich, R. L., Lu, X., Wang, Y.-P., & Oleksyn, J. (2014). Biogeographic variation in evergreen conifer needle longevity and impacts on boreal forest carbon cycle projections. *Proceedings of the National Academy of Sciences of the United States of America*, *111*, 13703–13708.
Robeson, S. M. (2015). Revisiting the recent California drought as an extreme value. *Geophysical Research Letters*, *42*, 6771–6779.
Robinson, D. (2001). δ15N as an integrator of the nitrogen cycle. *Trends in Ecology & Evolution*, *16*, 153–162.
Rocha, J. C., Peterson, G., Bodin, Ö., & Levin, S. (2018). Cascading regime shifts within and across scales. *Science*, *362*, 1379–1383.
Roebroek, C. T. J., Melsen, L. A., Hoek van Dijke, A. J., Fan, Y., & Teuling, A. J. (2020). Global distribution of hydrologic controls on forest growth. *Hydrology and Earth System Sciences*, *24*, 4625–4639.
Salzer, M. W., Larson, E. R., Bunn, A. G., & Hughes, M. K. (2014). Changing climate response in near-treeline bristlecone pine with elevation and aspect. *Environmental Research Letters*, *9*, 114007.
Sánchez-Salguero, R., Camarero, J. J., Gutiérrez, E., Rouco, F. G., Gazol, A., Sangüesa-Barreda, G., Andreu-Hayles, L., Linares, J. C., & Seftigen, K. (2017). Assessing forest vulnerability to climate warming using a process-based model of tree growth: Bad prospects for rear-edges. *Global Change Biology*, *23*, 2705–2719.
Shestakova, T. A., Camarero, J. J., Ferrio, J. P., Knorre, A. A., Gutiérrez, E., & Voltas, J. (2017). Increasing drought effects on five European pines modulate Δ13C-growth coupling along a Mediterranean altitudinal gradient. *Functional Ecology*, *31*, 1359–1370.
Slette, I. J., Post, A. K., Awad, M., Even, T., Punzalan, A., Williams, S., Smith, M. D., & Knapp, A. K. (2019). How ecologists define drought, and why we should do better. *Global Change Biology*, *25*, 3193–3200.
Speer, J. H. (2010). *Fundamentals of tree-ring research*. University of Arizona Press.
Steidinger, B. S., Crowther, T. W., Liang, J., Van Nuland, M. E., Werner, G. D. A., Reich, P. B., Nabuurs, G. J., de Miguel, S., Zhou, M., Picard, N., Herault, B., Zhao, X., Zhang, C., Routh, D., & Peay, K. G. (2019). Climatic controls of decomposition drive the global biogeography of forest-tree symbioses. *Nature*, *569*, 404–408.
Stephenson, N. (1998). Actual evapotranspiration and deficit: Biologically meaningful correlates of vegetation distribution across spatial scales. *Journal of Biogeography*, *25*, 855–870.
Stephenson, N. L. (1988). Classification and description of the montane and subalpine forest and woodland communities of sequoia National Park. Final contract report to the Sequoia Natural History Association.
Stephenson, N. L., Das, A. J., Ampersee, N. J., Bulaon, B. M., & Yee, J. L. (2019). Which trees die during drought? The key role of insect host-tree selection. *Journal of Ecology*, *107*, 2383–2401.
Sturm, J., Santos, M. J., Schmid, B., & Damm, A. (2022). Satellite data reveal differential responses of Swiss forests to unprecedented 2018 drought. *Global Change Biology*, *28*, 2956–2978.
Trenberth, K. E., Dai, A., van der Schrier, G., Jones, P. D., Barichivich, J., Briffa, K. R., & Sheffield, J. (2014). Global warming and changes in drought. *Nature Climate Change*, *4*, 17–22.
Tuomi, M., Thum, T., Järvinen, H., Fronzek, S., Berg, B., Harmon, M., Trofymow, J. A., Sevanto, S., & Liski, J. (2009). Leaf litter decomposition—Estimates of global variability based on Yasso07 model. *Ecological Modelling*, *220*, 3362–3371.
Tyukavina, O. N., Neverov, N. A., & Mineev, A. L. (2019). Variations in the length of Scots pine (*Pinus sylvestris* L.) needles under the influence of climatic factors and solar activity in different conditions of northern taiga. *Journal of Forest Science*, *65*, 313–320.
U.S. Fish & Wildlife Service. (2022). Endangered and threatened wildlife and plants; threatened species status with section 4(d) rule for Whitebark Pine (*Pinus albicaulis*), December 15. https://www.fws.gov/species-publication-action/endangered-and-threatened-wildlife-and-plants-threatened-species-70.
USDA Forest Service. (2020). WhitebarkPine_CA_2020_v1.

13652486, 2023, 15, Downloaded from https://onlinelibrary.wiley.com/doi/10.1111/gcb.16740 by National Forest Service Library, Wiley Online Library on [03/08/2023]. See the Terms and Conditions (https://onlinelibrary.wiley.com/terms-and-conditions) on Wiley Online Library for rules of use; OA articles are governed by the applicable Creative Commons License

USFS. (n.d.). Chapter 33-Ecological Subregions of the United States. https://www.fs.fed.us/land/pubs/ecoregions/ch33.html

Valor, T., Hood, S. M., Piqué, M., Larrañaga, A., & Casals, P. (2021). Resin ducts and bark thickness influence pine resistance to bark beetles after prescribed fire. *Forest Ecology and Management*, *494*, 119322.

van der Maaten-Theunissen, M., Kahle, H.-P., & van der Maaten, E. (2013). Drought sensitivity of Norway spruce is higher than that of silver fir along an altitudinal gradient in southwestern Germany. *Annals of Forest Science*, *70*, 185–193.

van Mantgem, P., Milano, E., Dudney, J., Nesmith, J., Vandergast, A. G., & Zald, H. (in review). Growth, drought response, and climate-associated genomic structure in whitebark pine in the Sierra Nevada of California. *Ecology and Evolution*.

Whittaker, R. J., Nogués-Bravo, D., Araújo, M. B., & Araújo, M. B. (2007). Geographical gradients of species richness: a test of the water-energy conjecture of Hawkins et al. (2003) using European data for five taxa. *Global Ecology and Biogeography*, *16*, 76–89.

Wong, C. M., & Daniels, L. D. (2017). Novel forest decline triggered by multiple interactions among climate, an introduced pathogen and bark beetles. *Global Change Biology*, *23*, 1926–1941.

Wood, S. (2022, February 24). Mgcv: Mixed GAM computation vehicle with automatic smoothness estimation.

Zald, H. S. J., Callahan, C. C., Hurteau, M. D., Goodwin, M. J., & North, M. P. (2022). Tree growth responses to extreme drought after mechanical thinning and prescribed fire in a Sierra Nevada mixed-conifer forest, USA. *Forest Ecology and Management*, *510*, 120107.

Zhai, L., Bergeron, Y., Huang, J.-G., & Berninger, F. (2012). Variation in intra-annual wood formation, and foliage and shoot development of three major Canadian boreal tree species. *American Journal of Botany*, *99*, 827–837.

SUPPORTING INFORMATION

Additional supporting information can be found online in the Supporting Information section at the end of this article.

How to cite this article: Dudney, J., Latimer, A. M., van Mantgem, P., Zald, H., Willing, C. E., Nesmith, J. C. B., Cribbs, J., & Milano, E. (2023). The energy–water limitation threshold explains divergent drought responses in tree growth, needle length, and stable isotope ratios. *Global Change Biology*, *29*, 4368–4382. https://doi.org/10.1111/gcb.16740

13652486, 2023, 15, Downloaded from https://onlinelibrary.wiley.com/doi/10.1111/gcb.16740 by National Forest Service Library, Wiley Online Library on [03/08/2023]. See the Terms and Conditions (https://onlinelibrary.wiley.com/terms-and-conditions) on Wiley Online Library for rules of use; OA articles are governed by the applicable Creative Commons License